Study on architecture design of electroactive sites on Vanadium Redox Flow Battery (V-RFB)

Suhailah Sujali[1], *Mohd Rusllim* Mohamed[1], *Ahmed Nurye* Oumer[2], *Azizan* Ahmad[3] and *Puiki* Leung[4]

[1]Faculty of Electrical and Electronics Engineering, Universiti Malaysia Pahang, 26600 Pekan, Pahang, MYS
[2]Faculty of Mechanical Engineering, Universiti Malaysia Pahang, 26600 Pekan, Pahang, MYS
[3]School of Chemical Sciences and Food Technology, Universiti Kebangsaan Malaysia 43600 Bangi, Selangor, MYS
[4]Department of Materials, University of Oxford, Oxford, OX1 3PH, UK

Abstract. Numerous researches have been conducted to look for better design of cell architecture of redox flow battery. This effort is to improve the performance of the battery with respect to further improves of mass transport and flow distribution of electroactive electrolytes within the cell. This paper evaluates pressure drop and flow distribution of the electroactive electrolyte in three different electrode configurations of vanadium redox flow battery (V-RFB) cell, namely square-, rhombus- and circular-cell designs. The fluid flow of the above-mentioned three electrode design configurations are evaluated under three different cases i.e. no flow (plain) field, parallel flow field and serpentine flow field using numerically designed three-dimensional model in Computational Fluid Dynamics (CFD) software. The cell exhibits different characteristics under different cases, which the circular cell design shows promising results for test-rig development with low pressure drop and better flow distribution of electroactive electrolytes within the cell. Suggestion for further work is highlighted.

1 Introduction

Energy storage is recognised as an important technology to work with variable and intermittent in nature of renewable power sources. Therefore, energy storage has been introduced to retain and sustain the required operational and system reliability of the power sources [1][2]

Through various energy storage technologies, vanadium redox flow battery (V-RFB) shown in Fig.1[3] offers a promise because of its unique features by providing effective and simple operation, capability of decoupling high power and energy, may operate at room temperature, fast response and recharging contenders. Furthermore it comprises an excellent chemical stability that shows an extremely long-round-trip cycle, have long discharge times, good in modular design, exhibits for highly reversible redox kinetics, enable the technology for large-scale applications with theoretically reasonable and controlled maintenance cost compared to conventional battery[1][4–7]

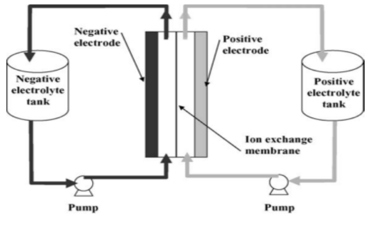

Fig. 1. Unit cell redox flow battery

As the name applies, flow battery is an electrochemical cell that produces electrical output through electrochemical reactions of two electrolytes that flow within the cell. Most of the researches in the past focused on improving poor kinetic reactions [8], conductivity [9], redox couples [10] electrodes [11] and battery characterisation [12]. A more recent works by Houser [13] *et al.* and Kumar [14] *et al.* were focusing on improving mass transport issues in redox flow battery. Mass flow is play an important role in battery to perform well [15][16]. The basic idea of study is to overcome the mass transport polarization issues and outcomes by introducing new design channel that may distribute the electrolyte well with reasonable pumping energy required. Recently, researchers systematically discuss about the electrode porous (electroactive sites) that acts as key in V-RFB systems[11][17][18].

In the conventional flow field of porous electrode, the electrolyte is directly pumped through the electroactive sites electrodes. This may results in unevenly distributed flow within the cell because the electrolyte flow through random pores of the electroactive sites part. This may causes pressure drop arising together with flow direction and this lead to a mass transfer losses and deterioration problems when the electrolyte flow into the electrode just from one lateral side. Previous researchers [19][20] have explored on creating new and appropriate flow channel for control the electrolyte flow and directly gives a positive feedback on improvement of V-RFB performance. There are literatures on several experimental and numerical investigation of the V-RFB design system. Xu *et al.* [19][21] proposed experimentally and numerical investigation on architecture of redox flow battery. The study focused on evaluation of vanadium redox flow battery performance based on flow of electrolytes within the cell, focusing on with and without flow field electrode configurations supported by experimental data and numerically designed three-dimensional model of V-RFB. The study concluded that energy efficiency of V-RFB is much higher by 5% when electroactive sites of flow field was applied as compared to energy efficiency without flow field.

Conversely, Wang *et al.* [22] studied on parallel flow design configurations concluded that energy efficiency of V-RFB could be further be enhanced by 5% in staggered arrangement as compared to symmetrical arrangement. Wang *et al.* claimed that design of flow field for V-RFBs is an important areas that needs more attention for further investigation and it was concluded that limited work in this area of research has been conducted. Fig.2 depicts different electrode configurations that have been used in previous studies, namely no flow flied (plain)-, parallel- and serpentine-electrode configurations.

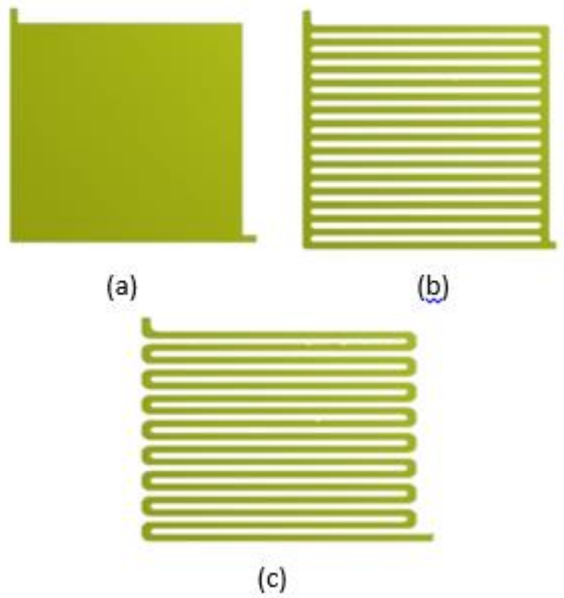

Fig. 2. Schematic drawing of three type of flow field (a) no flow flied- (b) parallel- (c) serpentine- configurations

On the other hand, Bortolin *et al.* [23] and Khor *et al.* [8] introduced a methodology included several performance indicators by using computational fluid dynamic simulation on determining the flow distribution in a particular geometry of V-RFB cell. Ressel *et al.* [24] studied the influence of different flow cell geometry design by introduced a tubular cell design with a flow by electrode configuration on the performance and system efficiency of V-RFB cell.

Based on the brief review, it is important to note that both flow field electrode configurations and architecture design of the cell play important roles for future advancement of flow battery technology.

Nevertheless, apart from Khor *et al.* which worked on rhombus shape electrode geometry design, all other highlighted studies were very much focused on square-shape based cell geometry design.

This study attempts to extend the works in both flow field electrode configurations and cell design geometry; looking into perspective of effect of flow distribution within three different cell design i.e. square shape, rhombus shape and circular shape electrode geometry design. The first part of studies were focused on identifying the best shape to be implemented in V-RFB cell design with respect to flow distribution within the cell based on no flow field electrode configurations. Extended works were focused on application of the best shape of electrode geometry design in further two electrode configurations to identify the lowest pressure drop which could resulted in better performance of the V-RFB.

2 Development of V-RFB cell in Computational Fluid Dynamics (CFD)

2.1. Simulation details

Numerical simulations were carried out and solved using the ANSYS 16.2 package with a combination of the self-written source terms in console zone. Three dimensional models were built in fluid flow (fluent) under analysis systems for handling the flow in the porous carbon electrode. The fluid model used is sulfuric acid solution diluted with vanadium oxides. The fluid was considered to be incompressible and isothermal, with density and dynamic viscosity were 1334.9 Kgm^{-3} and 0.0024 Pa respectively.

The model domains were developed based on a 100 cm^2 (10 cm x 10 cm) active sites of electrode with a thickness of 3 mm with 0.00424 m cross section area of the channel. The details operating parameter in geometry and setup parameter are shown in Table 1. This dynamic model were simulated with different velocity inlet condition that has been calculated analytically and a specified uniform flow velocity at the inlet and 0 Pa pressure at the outlet was set in the boundary condition. No slip condition on the walls and no flux condition were applied to the domain surfaces exceptional for inlet outlet flow channels. In all simulations, the fluent was set with double precision and pressure-based solver. The porous media model was evaluated with a pressure-velocity coupling algorithm SIMPLE (Semi Implicit Method for Pressure-Linked Equation) in solution methods. The CFD simulation were conducted at different flow rates, flow with/without distribution channel and with different electrode compartment design in order to evaluated the best configuration for transport phenomena and performance in the V-RFB.

Table 1 Operating parameters of CFD simulation of 100 cm^2 V-RFB cell

Parameters	Symbols	Value	Unit	Ref
Electrode thickness	δ_e	3	mm	

Electrode height	h	100	mm	
Electrode width	w	100	mm	
Polymer electrolyte membrane	δ_{mem}	3	mm	
Operating temperature	T	288	K	
Electrode porosity	ε_0	0.7	ι	[21]
Electrode fiber diameter	d_f	17.6	μm	
Electrolyte volumetric flowrate	Q	5, 10,15, 20, 25,30	cm^3s^{-1}	
Electrolyte density	ρ	1334.9	Kg m^{-3}	
Electrolyte kinematic viscosity	v	$3.2x10^{-6}$	m^2s^{-1}	
Carman-kozeny constant	K_{CK}	5.55		[21]
Carbon density	ρ	2240	Kg m^{-3}	
Specific heat of carbon	$c\rho$	710	$Jkg^{-1}K^{-1}$	
Thermal conductivity of carbon		0.2	$Wm^{-1}K^{-1}$	
Vanadium concentration	c	1.6	mol m^{-3}	
Electrolyte dynamic viscosity	μ	0.0024	Kg m^{-s}	
Thermal conductivity of electrolyte		0.67	$Wm^{-1}K^{-1}$	
Reservoir volume	V_C	200	ml	
Rib width		3	mm	
No of channels/bends		16		

2.2 Pressure drops in cell

Pressure drop is a crucial issue in the system for determining the smooth continuous flow circulation of the liquids inside the cell stack. At variance of flow pattern design in the cell electrode (active area) may give a different flow distribution and pressure drop. In this study, two conditions were set; at lower flow rate, the flow was consider laminar flow whereas higher flow rate was considered as turbulent flow. This consideration of flow was supported by the calculation by referring Reynolds number formulae.

The Reynolds number were determined respectively are shown in Equation 1. In this paper, various flow pattern design were considered including without distribution channel (direct feeding) in a porous media electrode and indirect feeding channel; a parallel and serpentine pattern.

$$Re_{efb} = \frac{\rho_{efb} VD}{\mu_{efb}} \quad (1)$$

Pressure drop result is shown for a pumping energy required in a redox flow battery cell. The lesser pressure drop of the cell battery, the lower consumption of pumping energy needed. At variance of flow pattern design in the cell electrode (active area) may give a different flow distribution and pressure drop. Differential pressure (Δρ) is a pressure between inlet and outlet (over the length of the electrode, L), and this result comes from the relationship of the viscous resistance flow, permeability of the electrode material and viscosity of the electrolyte. A pressure drop through this electrode can be resolved according to the Darcy's Law by including a flow rate (Q) and viscosity of the electrolyte (η_e) also as shown in Equation 2:

$$\Delta P = \frac{\eta_e}{K_e(\varepsilon)} Q . \frac{L}{A} \quad (2)$$

The permeability (K_e) is dependent on the porosity of the electroactive sites of carbon electrode. Flow cross-sectional area (A) changes with different cell geometry (active sites).

2.3 Computational domains and boundary conditions

A symmetry boundary condition were elucidated to set the operational point of V-RFB cell that consist of inlet velocity magnitude, gauge-pressure at outlet region, symmetry planes and wall condition surface .The no-slip boundary condition was applied on the electroactive sites of the electrode excluded the inlet and outlet regions. Next, on the solution method setup part, pressure-velocity coupling was selected and performed by the SIMPLE algorithm and the second-order upwind scheme was used in a computational domain. Finally, numerical analysis were simulated through continues running by maintaining a steady state conditions of the operation of the battery cell and mass-weighted values applied also monitored.

3 Result and Discussions

With the aim to investigate the influence of the cell's electrode geometry design on flow distribution within the cell, flow rates at 5 $cm^3 s^{-1}$ to 30 $cm^3 s^{-1}$ were fed into three proposed 100 cm^2 square shape, rhombus shape and circular shape electrode geometry design. Fig. 3 indicates the shapes plays significant parts affecting the flow distribution within the three proposed electrode geometry designs when applied through no flow field (plain) electrode configuration at flow rate of 30 $cm^3 s^{-1}$. The result shows that circular shape design gives the best uniformity electrolyte distribution as compared to square shape and rhombus shape electrode geometry design. Other results for different flow rates will be published in forthcoming extended paper.

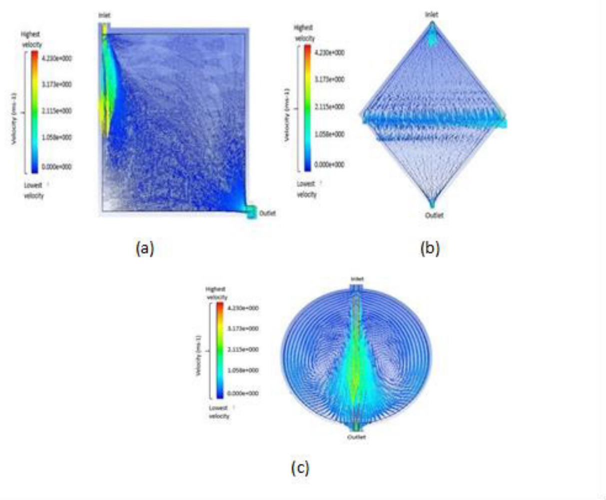

Fig. 3 Velocity vector shows flow distribution for 100 cm^2 three different geometrical cell design at same 30 cm^3 s^{-1} flow rates applied (a) square cell (b) rhombus cell (c) Circular cell

Moreover, pumping power is one of the impact parameter for determining a better RFB system. It should be noted that, lower pressure drop indicates a low pumping consumption. In this study, pressure drop has been calculated to determine which proposed geometrical cell design consume a lesser pumping power. In this case, area-weighted average of static pressure has been computed for each geometrical designs. Fig. 4 shows the pressure drop for each geometrical designs at various flow rate of 5 cm^3 s^{-1} until 30 cm^3 s^{-1}. It should be noted that, the flow rate increases in accordance to applied flow rate, indicating of uniform distribution of electrolytes within the cell with the expense of higher pumping losses; higher pumping power required is proportional to higher pumping losses which could affecting in overall efficiency of V-RFB system. The results shows that the square flow frame has the highest pressure drop (17.3 KPa) at flow rates 30 cm^3s^{-1}, followed by rhombus cell (16.5 KPa) and circular shape is (12.2 KPa).

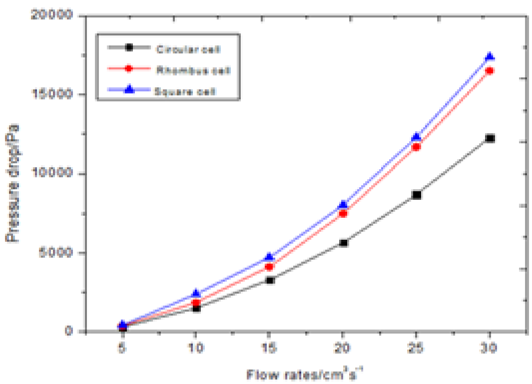

Fig. 4. Comparison of pressure drop within the three different 100 cm^2 geometrical cell designs i.e. square shape, rhombus shape and circular shape cell geometry design at various flow rate of 5 cm^3 s^{-1} until 30 cm^3 s^{-1}

Furthermore, with circular shape cell design represent best result for both flow distribution and pressure drop at various flow rates, the study is extended to determine which flow field configurations would be the best to be applied on 100 cm^2 circular shape cell design.

Fig.5 represents the pressure drops for no flow field porous medium model and two different flow pattern at the flow rates 5 cm^3 s^{-1} until 30 cm^3 s^{-1}. The result of the numerical simulation indicates that the parallel flow field shows the lowest pressure drop at 253 Pa whereas the no flow field and the serpentine distribution channel has represented a 422 Pa and 2469 Pa pressure drop. This indicates that serpentine flow channel has a highest pressure drops and no flow field design is two times higher than parallel design. By comparing the parallel and no flow field designs, it should be noted that at lowest flow rates, by adding flow field at bipolar plates it can significantly reduce a pressure drop. Nevertheless, when the flow rate is increased, for example of 30 cm^3 s^{-1}, the pressure drop for the porous electrode and two types of flow patterns increase accordingly as shown in Fig.5. For the first two fields, the pressure drop increases from 253 to 12432 Pa and from 2469 Pa to 45701 Pa respectively whereas without flow field electrode it increases from 422 Pa to 17375 Pa. Details data of effect on pressure drops for respective square shape, rhombus shape and circular shape cell geometry design with respect to flow rates 5 cm^3 s^{-1} until 30 cm^3 s^{-1} will be discussed in forthcoming paper.

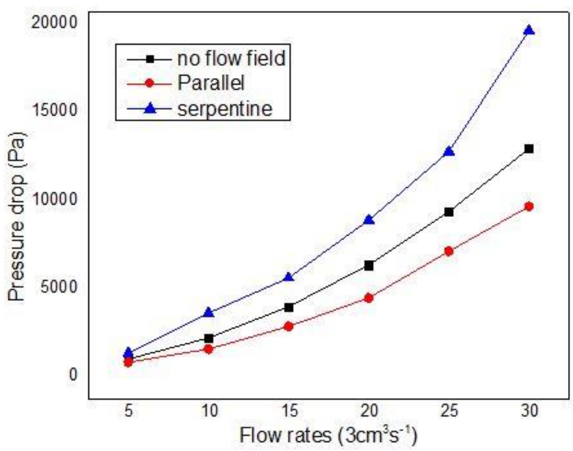

Fig. 5. Computationally pressure drop data for no flow field, parallel- (c) serpentine-configurations for 100 cm^2 circular shape cell geometry design with respect to flow rates 5 cm^3 s^{-1} until 30 cm^3 s^{-1}

4 Conclusions

This study demonstrates that the circular shape cell geometry design has most uniform electrolyte distribution within the cell at applied 30 cm^3 s^{-1} flow rates as well as lowest average pressure drop as compared to square and rhombus cell design counterparts, whereas parallel flow field configurations represents the best options for 100 cm^2 circular shape cell geometry design of V-RFB at 5 cm^3 s^{-1} - 30 cm^3 s^{-1} flow rates. Further works on effect of cell architectures to the performance of V-RFB with respect to coulombic, voltage and energy efficiency will be discussed in forthcoming paper.

Acknowledgements

This work was supported by Malaysia's Ministry of Education (MOE) - Fundamental Research Grant Scheme (FRGS) - RDU 150123, Research Acculturation Collaborative Effort (RACE) - RDU151316 and Postgraduate Research Scheme - PGRS170352, Universiti Malaysia Pahang.

References

1. M. Guarnieri, P. Mattavelli, G. Petrone, and G. Spagnuolo, "Vanadium Redox Flow Batteries," no. december 2016, pp. 20–31, 1932.
2. T. M. I. Mahlia, T. J. Saktisahdan, A. Jannifar, M. H. Hasan, and H. S. C. Matseelar, "A review of available methods and development on energy storage; Technology update," *Renew. Sustain. Energy Rev.*, vol. 33, pp. 532–545, 2014.
3. C. P. De Le and F. C. Walsh, "Redox flow cells for energy conversion," vol. 160, pp. 716–732, 2006.
4. M. Rusllim Mohammad, S. M. Sharkh, and F. C. Walsh, "Redox flow batteries for hybrid electric vehicles: progress and challenges," *2009 IEEE Veh. Power Propuls. Conf.*, no. August 2016, pp. 551–557, 2010.
5. A. Z. Weber, M. M. Mench, J. P. Meyers, P. N. Ross, J. T. Gostick, and Q. Liu, "Redox flow batteries: A review," *J. Appl. Electrochem.*, vol. 41, no. 10, pp. 1137–1164, 2011.
6. G. R. Fisher, M. Ieee, M. R. Anstey, V. V Viswanathan, and M. L. Perry, "Redox Flow Batteries : An Engineering Perspective," pp. 1–24, 2014.
7. T. Jyothi Latha and S. Jayanti, "Hydrodynamic analysis of flow fields for redox flow battery applications Batteries," *J. Appl. Electrochem.*, vol. 44, no. 9, pp. 995–1006, 2014.
8. A. C. Khor *et al.*, "Numerical investigation on serpentine flow field and rhombus electrolyte compartment of vanadium redox flow battery (V-RFB)," *ARPN J. Eng. Appl. Sci.*, vol. 11, no. 10, 2016.
9. T. Mohammadi, "Characterisation of novel composite membrane for redox flow battery applications," vol. 98, pp. 77–87, 1995.
10. P. K. Leung, M. R. Mohamed, A. A. Shah, Q. Xu, and M. B. Conde-duran, "A mixed acid based vanadium e cerium redox fl ow battery with a zero-gap serpentine architecture," vol. 274, pp. 651–658, 2015.
11. P. Leung, J. Palma, E. Garcia-quismondo, L. Sanz, M. R. Mohamed, and M. Anderson, "Evaluation of electrode materials for all-copper hybrid fl ow batteries," *J. Power Sources*, vol. 310, pp. 1–11, 2016.
12. M. R. Mohamed, P. K. Leung, and M. H. Sulaiman, "Performance characterization of a vanadium redox flow battery at different operating parameters under a standardized test-bed system," *Appl. Energy*, vol. 137, pp. 402–412, 2015.
13. J. Houser, A. Pezeshki, J. T. Clement, D. Aaron, and M. M. Mench, "Architecture for improved mass transport and system performance in redox fl ow batteries," *J. Power Sources*, vol. 351, pp. 96–105, 2017.
14. S. Kumar and S. Jayanti, "Effect of flow field on the performance of an all-vanadium redox flow battery," *J. Power Sources*, vol. 307, pp. 782–787, 2016.
15. X. Ma, H. Zhang, C. Sun, Y. Zou, and T. Zhang, "An optimal strategy of electrolyte flow rate for vanadium redox flow battery," *J. Power Sources*, vol. 203, pp. 153–158, 2012.
16. A. Tang, J. Bao, and M. Skyllas-Kazacos, "Studies on pressure losses and flow rate optimization in vanadium redox flow battery," *J. Power Sources*, vol. 248, pp. 154–162, 2014.
17. a C. Khor, M. R. Mohamed, M. H. Sulaiman, and M. R. Daud, "Packaging Improvement for Unit Cell Vanadium Redox Flow Battery (V-RFB)," no. 6, pp. 808–811, 2014.
18. C. Blanc, S. Member, and I. A. Rufer, "Multiphysics and Energetic Modeling of a Vanadium Redox Flow Battery," 2008.
19. Q. Xu, T. S. Zhao, and C. Zhang, "Performance of a vanadium redox flow battery with and without flow fields," *Electrochim. Acta*, vol. 142, pp. 61–67, 2014.
20. D. H. Jeon, S. Greenway, S. Ã. Shimpalee, and J. W. Van Zee, "The effect of serpentine flow-field designs on PEM fuel cell performance," vol. 33, pp. 1052–1066, 2008.
21. Q. Xu, T. S. Zhao, and P. K. Leung, "Numerical investigations of flow field designs for vanadium redox flow batteries," *Appl. Energy*, vol. 105, pp. 47–56, 2013.
22. Q. Wang, Z. G. Qu, Z. Y. Jiang, and W. W. Yang, "Numerical study on vanadium redox fl ow battery performance with non- uniformly compressed electrode and serpentine fl ow fi eld," vol. 220, no. September 2017, pp. 106–116, 2018.
23. S. Bortolin, P. Toninelli, D. Maggiolo, M. Guarnieri, and D. Del Col, "CFD study on electrolyte distribution in redox flow batteries," *J. Phys. Conf. Ser.*, vol. 655, no. November, p. 12049, 2015.
24. S. Ressel, A. Laube, S. Fischer, A. Chica, T. Flower, and T. Struckmann, "Performance of a vanadium redox fl ow battery with tubular cell design," *J. Power Sources*, vol. 355, pp. 199–205, 2017